



Cite this: *Chem. Commun.*, 2015, 51, 12966

Received 19th May 2015,
Accepted 1st July 2015

DOI: 10.1039/c5cc04123f

www.rsc.org/chemcomm

A new Ru^{II}Rh^{III} bimetallic with a single Rh–Cl bond as a supramolecular photocatalyst for proton reduction†

Rongwei Zhou,* Gerald F. Manbeck,‡ Dexter G. Wimer and Karen J. Brewer§

A new Ru^{II}Rh^{III} structural motif [(bpy)₂Ru(dpp)RhCl(tpy)]⁴⁺ with one halide on the Rh^{III} center demonstrates light-driven proton reduction ability, establishing that two halide ligands are not mandatory despite all prior systems containing a *cis*-RhCl₂ catalytic site. This new design provides a novel approach to modulate Rh^{III} redox behavior and catalytic activity with insight into catalytic intermediates.

Solar water splitting to generate H₂ has gained considerable interest as a method to produce an alternative fuel to meet future energy demands.¹ Robust systems that absorb visible light, facilitate electron transfer and catalyze H₂ formation are required for achieving solar energy conversion. To this end, supramolecular complexes incorporating separate units with individual properties offering unique functions to the entire molecule have been designed.² In contrast to the bimolecular electron transfer (ET) reactions in the multi-component photocatalytic water reduction systems developed in the 1970s,³ the supramolecular approach exploits intramolecular ET. Supramolecular complexes coupling metal-based chromophores to a catalytic center photocatalytically reduce water to H₂ under various conditions.⁴ Impediments to engineering supramolecular complexes for solar H₂ production include the small number of molecular systems capable of photochemically collecting reducing equivalents and the lack of fundamental understanding of multielectron photochemistry.

In seeking an efficient and robust supramolecular photocatalyst, a series of Ru^{II}Rh^{III}-containing supramolecular complexes coupling polypyridyl Ru^{II} chromophores to a Rh^{III} catalytic center *via* a bridging ligand dpp (2,3-bis(2-pyridyl)pyrazine)

were explored. The first photocatalyst of this type, [(bpy)₂Ru(dpp)₂RhCl₂](PF₆)₅, inspired the development of Ru^{II}Rh^{III}Ru^{II} trimetallics with the architecture of [(TL)₂Ru(dpp)₂RhX₂](PF₆)₅ (TL = bpy, 1,10-phenanthroline (phen), or 4,7-diphenyl-1,10-phenanthroline (Ph₂phen); X = Cl or Br) to explore factors that control photoinitiated electron collection (PEC) and catalytic activity.^{4f,5} The presence of a Rh(dσ*)-based LUMO (lowest unoccupied molecular orbital) in the Ru^{II}Rh^{III}Ru^{II} complexes is a key energetic requirement for PEC at the Rh^{III} catalytic center.⁶ PEC on the Rh^{III} center forms the proposed active species, Ru^{II}Rh^IRu^{II}, upon sequential reductive quenching of the ³MLCT (metal-to-ligand charge transfer) excited state by a sacrificial electron donor.^{6b} Recent studies also show that two Ru^{II} chromophores are not required for photocatalysis. Active Ru^{II}Rh^{III} bimetallics require a Rh-based LUMO and steric protection around the photo-generated Rh^I center to prevent dimerization that leads to catalytic deactivation.^{4g} These Ru^{II}Rh^{III}Ru^{II} and Ru^{II}Rh^{III} motifs represent homogenous single-component photocatalysts for H₂ generation.

To the best of our knowledge, all reported dpp-bridged Ru^{II}Rh^{III} and Ru^{II}Rh^{III}Ru^{II} photocatalysts have two labile halide ligands (Cl or Br) on the Rh^{III} center. Here we propose the replacement of one halide ligand with an N donor of a polypyridyl ligand as a means to (1) modulate the electrochemical properties of the catalytic Rh center, (2) test the hypothesis that only one labile halide ligand is needed in the dpp-bridged Ru^{II}Rh^{III} pre-catalyst for photocatalytic water reduction, (3) expand the scope of structural designs for competent Rh-containing supramolecular photocatalysts, and (4) provide a new mechanism of steric protection of the Rh^I center.

The ligand tpy (2,2':6',2''-terpyridine) has been widely used in coordination chemistry with meridional tridentate (η³) chelation being the most common coordination mode. Taking advantage of the tridentate binding mode, the new Ru^{II}Rh^{III} complex, [(bpy)₂Ru(dpp)RhCl(tpy)](PF₆)₄ (Ru^{II}Rh^{III}Cl(tpy)), has been prepared to test the hypotheses described above. For comparative purposes, we have studied the *cis*-Rh^{III}Cl₂ analogue [(bpy)₂Ru(dpp)RhCl₂(bpy)](PF₆)₃ (Ru^{II}Rh^{III}Cl₂(bpy)). Herein we report the electrochemical, photochemical, and catalytic properties

Department of Chemistry, Virginia Tech, Blacksburg, VA, 24061-0212, USA.

E-mail: rowezhou@vt.edu

† Electronic supplementary information (ESI) available: Detailed synthesis; coupled CVs before and after control potential electrolysis; ESI mass spectra of products after control potential electrolysis; and the profile of the photolysis of hydrogen production. See DOI: 10.1039/c5cc04123f

‡ Current address: Chemistry Department, Brookhaven National Laboratory, Upton, NY 11973-5000, USA.

§ Karen J. Brewer deceased October 24, 2014.



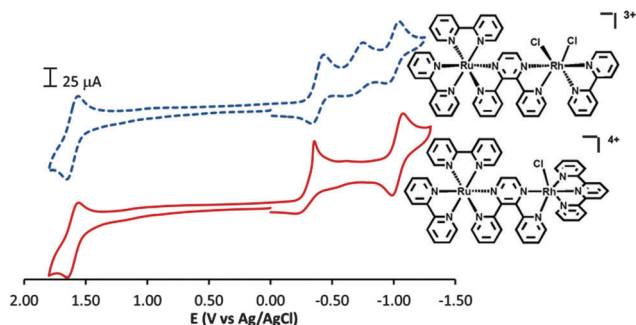


Fig. 1 CVs and structures of $\text{Ru}^{\text{II}}\text{Rh}^{\text{III}}\text{Cl}_2(\text{bpy})$ (blue dashed) and $\text{Ru}^{\text{II}}\text{Rh}^{\text{III}}\text{Cl}(\text{tpy})$ (red solid) in 0.1 M Bu_4NPF_6 acetonitrile.

of these two RuRh supramolecular complexes. It was found that $\text{Ru}^{\text{II}}\text{Rh}^{\text{III}}(\text{tpy})$ is an active photocatalyst for H_2 production. The results suggested that two Rh–Cl bonds were not required for photocatalysis. All synthetic details, including ^1H NMR spectra, are provided in the ESI† (Fig. S1–S3).

Cyclic voltammetry (CV) was utilized to investigate the influence of TL variation on the redox properties of the Rh^{III} center. Fig. 1 shows that both complexes possess a reversible $\text{Ru}^{\text{III/II}}$ couple at a similar potential (*ca.* 1.60 V vs. Ag/AgCl) indicating that the $\text{Ru}(\text{d}\pi)$ orbital energy is insensitive to the variation of the remote TL on Rh^{III} . Reductively, $\text{Ru}^{\text{II}}\text{Rh}^{\text{III}}\text{Cl}_2(\text{bpy})$ shows a quasi-reversible $\text{Rh}^{\text{III/II}}$ couple at -0.43 V ($\Delta E = 60$ mV), an irreversible $\text{Rh}^{\text{III/I}}$ couple at $E_p^c = -0.79$ V, and a reversible $\text{dpp}^{0/-}$ at -1.01 V. The assignments are confirmed by coulometric experiments and consistent with $[(\text{bpy})_2\text{Ru}(\text{dpp})\text{RhCl}_2(\text{phen})]^{3+}$.⁷ In $\text{Ru}^{\text{II}}\text{Rh}^{\text{III}}\text{Cl}(\text{tpy})$, the first reduction appears as an irreversible wave at $E_p^c = -0.35$ V vs. Ag/AgCl and comprises $2e^-$ /molecule. The appearance of the $2\text{Cl}^-/\text{Cl}_2$ oxidation couple in the CV of the reduced solution (Fig. S4, ESI†) suggests the dissociation of the Cl^- ligand from Rh^{III} upon reduction, providing an assignment of $\text{Rh}^{\text{III/II/I}}$ for the first reduction. Unlike $\text{Ru}^{\text{II}}\text{Rh}^{\text{III}}\text{Cl}_2(\text{bpy})$, very little current is seen in the anodic wave associated with the first reduction even upon increasing the scan rate to 1.0 V s^{-1} (Fig. S5, ESI†), establishing that Cl^- loss is faster in the tpy complex than the bpy complex. The $\text{Ru}^{\text{II}}\text{Rh}^{\text{III}}\text{Cl}(\text{tpy})$ geometry requires the Cl^- ligand to be *trans* to dpp whereas $\text{Ru}^{\text{II}}\text{Rh}^{\text{III}}\text{Cl}_2(\text{bpy})$ has one Cl^- *trans* to dpp and one Cl^- *trans* to bpy. This uncovers an important consideration in controlling the rate of halide loss critical to providing an active site in the reduced Rh^{I} species. The single $\text{Rh}^{\text{III/II/I}}$ couple in $\text{Ru}^{\text{II}}\text{Rh}^{\text{III}}\text{Cl}(\text{tpy})$ is in marked contrast to two separate Rh reductions in $\text{Ru}^{\text{II}}(\text{cis-Rh}^{\text{III}}\text{Cl}_2)$ bimetallics. The effect is traced to rapid halide loss and instability of the $1e^-$ reduced species of $\text{Ru}^{\text{II}}\text{Rh}^{\text{III}}\text{Cl}(\text{tpy})$ toward disproportionation whereas the $1e^-$ reduced $\text{Ru}^{\text{II}}\text{Rh}^{\text{III}}\text{Cl}_2(\text{bpy})$ likely possesses dpp^{*-} character and is comparatively more stable. The Ru-based first oxidation and Rh-based first reduction establish the $\text{Ru}(\text{d}\pi)$ HOMO and the $\text{Rh}(\text{d}\sigma^*)$ LUMO in both complexes with a lowest-lying MMCT (metal-to-metal charge transfer) excited state predicted to undergo PEC at the Rh^{III} center producing active photocatalysts.

The electronic absorption spectra of $\text{Ru}^{\text{II}}\text{Rh}^{\text{III}}\text{Cl}(\text{tpy})$ and $\text{Ru}^{\text{II}}\text{Rh}^{\text{III}}\text{Cl}_2(\text{bpy})$ are provided in Fig. S6 (ESI†). The UV spectrum

is dominated by intense ligand centered $\pi \rightarrow \pi^*$ transitions. $\text{Ru}^{\text{II}}\text{Rh}^{\text{III}}\text{Cl}(\text{tpy})$ displays a higher absorption intensity ($\epsilon = 74\,200$ M^{-1} cm^{-1}) at 280 nm than $\text{Ru}^{\text{II}}\text{Rh}^{\text{III}}\text{Cl}_2(\text{bpy})$ ($\epsilon = 59\,300$ M^{-1} cm^{-1}). A broad band between 400 and 500 nm is $^1\text{MLCT}$ in character with lower energies attributed to $\text{Ru}(\text{d}\pi) \rightarrow \text{dpp}(\pi^*)$ $^1\text{MLCT}$ transitions and higher energies attributed to $\text{Ru}(\text{d}\pi) \rightarrow \text{bpy}(\pi^*)$ $^1\text{MLCT}$ transitions. The spectra of the two bimetallics are nearly identical in the visible region, indicating that the structural difference at Rh does not impact the Ru^{II} $^1\text{MLCT}$ transitions.

Emission spectroscopy was used to investigate the photo-physical properties of these $\text{Ru}^{\text{II}}\text{Rh}^{\text{III}}$ complexes. The emission spectra of $\text{Ru}^{\text{II}}\text{Rh}^{\text{III}}\text{Cl}_2(\text{bpy})$, $\text{Ru}^{\text{II}}\text{Rh}^{\text{III}}\text{Cl}(\text{tpy})$, and a model complex $[(\text{bpy})_2\text{Ru}_2(\text{dpp})](\text{PF}_6)_4$ were recorded at room temperature (Fig. S7, ESI†) and 77 K (Table S1, ESI†). Both $\text{Ru}^{\text{II}}\text{Rh}^{\text{III}}$ complexes are weak emitters at room temperature from the $^3\text{MLCT}$ state ($\lambda_{\text{em}}^{\text{max}} = 750$ nm, $\Phi_{\text{em}} = 1.3 \times 10^{-4}$, $\tau = 40$ ns for $\text{Ru}^{\text{II}}\text{Rh}^{\text{III}}\text{Cl}_2(\text{bpy})$; $\Phi_{\text{em}} = 6.5 \times 10^{-5}$, $\tau = 30$ ns for $\text{Ru}^{\text{II}}\text{Rh}^{\text{III}}\text{Cl}(\text{tpy})$) and are dramatically quenched compared to the model complex $[(\text{bpy})_2\text{Ru}_2(\text{dpp})](\text{PF}_6)_4$ ($\Phi_{\text{em}} = 8.9 \times 10^{-4}$, $\tau = 130$ ns). The quenching is due to intramolecular electron transfer from dpp to Rh to populate the $^3\text{MMCT}$ excited state. Using k_r and k_{nr} from this model complex, k_{et} was obtained as 2.6×10^7 s^{-1} for $\text{Ru}^{\text{II}}\text{Rh}^{\text{III}}\text{Cl}(\text{tpy})$ and 1.7×10^7 s^{-1} for $\text{Ru}^{\text{II}}\text{Rh}^{\text{III}}\text{Cl}_2(\text{bpy})$. Intramolecular ET is impeded at 77 K and results in a long-lived $^3\text{MLCT}$ emission. At 77 K in an ethanol/methanol (4 : 1, v/v) glass matrix, the emissions of $\text{Ru}^{\text{II}}\text{Rh}^{\text{III}}\text{Cl}(\text{tpy})$ and $\text{Ru}^{\text{II}}\text{Rh}^{\text{III}}\text{Cl}_2(\text{bpy})$ are blue-shifted to 715 nm (λ_{max}) with a dramatic increase in the intensity and lifetime ($\tau = 2.3$ μs for $\text{Ru}^{\text{II}}\text{Rh}^{\text{III}}\text{Cl}_2(\text{bpy})$ and 2.1 μs for $\text{Ru}^{\text{II}}\text{Rh}^{\text{III}}\text{Cl}(\text{tpy})$) comparable to 2.4 μs for the model.

Spectrophotocatalytic and spectroelectrochemical analyses of the title $\text{Ru}^{\text{II}}\text{Rh}^{\text{III}}$ complexes demonstrated PEC at the Rh^{III} center. PEC is essential for $\text{Ru}^{\text{II}}\text{Rh}^{\text{III}}$ systems to provide active photocatalysts. Fig. 2 and Fig. S8 (ESI†) illustrate spectroscopic changes which accompany reduction at -0.65 V for $\text{Ru}^{\text{II}}\text{Rh}^{\text{III}}\text{Cl}(\text{tpy})$ and -0.95 V vs. Ag/AgCl for $\text{Ru}^{\text{II}}\text{Rh}^{\text{III}}\text{Cl}_2(\text{bpy})$ to generate the Rh^{I} species. The changes upon reduction are analogous to the changes upon the photolysis of $\text{Ru}^{\text{II}}\text{Rh}^{\text{III}}\text{Cl}(\text{tpy})$ and $\text{Ru}^{\text{II}}\text{Rh}^{\text{III}}\text{Cl}_2(\text{bpy})$ in the presence of *N,N*-dimethylaniline (DMA), establishing both complexes as molecular devices for PEC. Upon reduction, the $\text{Ru}(\text{d}\pi) \rightarrow \text{dpp}(\pi^*)$ $^1\text{MLCT}$ transitions blue shift, consistent with dpp bound to electron rich Rh^{I} . Reduction of Rh^{III} is

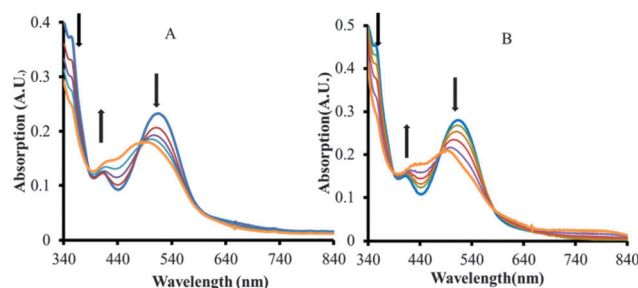


Fig. 2 Electronic absorption spectra generated from the electrochemical reduction (A, reduced at -0.65 V vs. Ag/AgCl) and photochemical reduction (B) of $\text{Ru}^{\text{II}}\text{Rh}^{\text{III}}\text{Cl}(\text{tpy})$ in deoxygenated acetonitrile at room temperature.

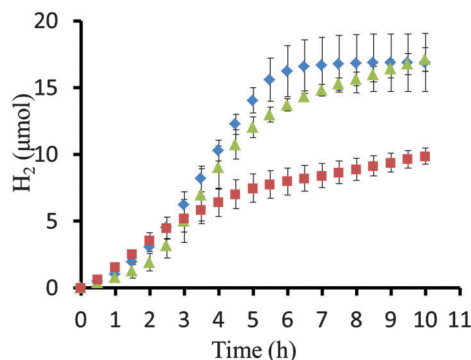


Fig. 3 Photocatalytic H_2 production of $\text{Ru}^{\text{II}}\text{Rh}^{\text{III}}\text{Cl}(\text{tpy})$ (65 μM) in acetone (blue diamond), DMF (green triangle), and CH_3CN (red square) solution with 1.5 M DMA and 0.6 M H_2O irradiated under 470 nm LED (light flux = $(2.36 \pm 0.05) \times 10^{19}$ photons per min).

accompanied by halide loss as the $\text{Rh}^{\text{I}}(\text{d}^8)$ reduces its coordination number to adopt a square planar geometry. This demonstration of PEC establishes $\text{Ru}^{\text{II}}\text{Rh}^{\text{III}}\text{Cl}(\text{tpy})$ as the first $\text{Ru}^{\text{II}}\text{Rh}^{\text{III}}$ system that undergoes PEC where the Rh^{III} is coordinated to a single halide, removing the previously employed design constraint that two coordinated halides are needed to promote PEC in $\text{Ru}^{\text{II}}\text{Rh}^{\text{III}}$ supramolecules as well as greatly expanding the potential supramolecular motifs available as single-component photocatalysts for proton reduction to produce H_2 fuel.⁵

Reductive quenching of the $^3\text{MLCT}$ excited state by DMA ($E(\text{DMA}^{+/0}) = 0.86$ V vs. Ag/AgCl) is reported as the primary pathway to generate $\text{Ru}^{\text{II}}\text{Rh}^{\text{I}}$ during the photolysis of $\text{Ru}^{\text{II}}\text{Rh}^{\text{III}}$.⁸ Using the ground state reduction potential, $E(\text{CAT}^{n+}/\text{CAT}^{(n-1)+})$, of 0.35 V for $\text{Ru}^{\text{II}}\text{Rh}^{\text{III}}\text{Cl}(\text{tpy})$ and 0.43 V for $\text{Ru}^{\text{II}}\text{Rh}^{\text{III}}\text{Cl}_2(\text{bpy})$, and $E^{0,0}$ estimated from $\lambda_{\text{em}}^{\text{max}}$ (77 K) as 1.73 eV, the thermodynamic driving force for reductive quenching, E_{redox} , is determined to be 0.52 V for $\text{Ru}^{\text{II}}\text{Rh}^{\text{III}}\text{Cl}(\text{tpy})$ and 0.44 V for $\text{Ru}^{\text{II}}\text{Rh}^{\text{III}}\text{Cl}_2(\text{bpy})$.^{5c} This driving force demonstrates that reduction of $\text{Ru}^{\text{II}}\text{Rh}^{\text{III}}$ to $\text{Ru}^{\text{II}}\text{Rh}^{\text{II}}$ using DMA is thermodynamically favorable. Quenching of the new $\text{Ru}^{\text{II}}\text{Rh}^{\text{III}}\text{Cl}(\text{tpy})$ is more favorable than $\text{Ru}^{\text{II}}\text{Rh}^{\text{III}}\text{Cl}_2(\text{bpy})$ and $[(\text{bpy})_2\text{Ru}(\text{dpp})]_2\text{RhCl}_2(\text{PF}_6)_5$ (0.49 V).^{5c} Greater driving force for reductive quenching facilitates the formation of the Rh^{I} active species and is hypothesized to enhance the photochemical reactivity for proton reduction.

Photocatalytic H_2 production from water–organic mixtures using $\text{Ru}^{\text{II}}\text{Rh}^{\text{III}}\text{Cl}(\text{tpy})$ was studied to test the hypothesis that two photolabile halides are not necessary for H_2 generation in the dpp-bridged $\text{Ru}^{\text{II}}\text{Rh}^{\text{III}}$ photocatalysts. As shown in Fig. 3, in CH_3CN $\text{Ru}^{\text{II}}\text{Rh}^{\text{III}}\text{Cl}(\text{tpy})$ produced 9.8 μmol H_2 with a TON of 33 and an overall quantum efficiency of 0.08% in 10 hours. Photocatalytic H_2 production was also observed in DMF and acetone with ca. 17 μmol H_2 and a TON of 58 showing improvements relative to strongly ligating CH_3CN .^{4h}

Photocatalytic H_2 production by $\text{Ru}^{\text{II}}\text{Rh}^{\text{III}}\text{Cl}_2(\text{bpy})$ and trimetallic $[(\text{bpy})_2\text{Ru}(\text{dpp})]_2\text{RhCl}_2(\text{PF}_6)_5$ was also conducted in DMF and CH_3CN for comparison (Fig. S10 and S11, ESI†). The catalytic activity of $\text{Ru}^{\text{II}}\text{Rh}^{\text{III}}\text{Cl}(\text{tpy})$ is better than $\text{Ru}^{\text{II}}\text{Rh}^{\text{III}}\text{Cl}_2(\text{bpy})$ and comparable to $[(\text{bpy})_2\text{Ru}(\text{dpp})]_2\text{RhCl}_2(\text{PF}_6)_5$ under similar conditions (Table S2, ESI†). The $\text{Ru}^{\text{II}}\text{Rh}^{\text{I}}$ state is proposed as

the active species for proton reduction.⁶ For $\text{Ru}^{\text{II}}\text{Rh}^{\text{III}}\text{Cl}_2(\text{bpy})$, electrochemical reduction leads to the formation of $[(\text{bpy})_2\text{Ru}(\text{dpp})\text{Rh}^{\text{I}}(\text{bpy})]^{3+}$ following halides loss, confirmed by ESI mass spectrometry ($m/z = 302.3$; calcd = 302.3, $M = [(\text{bpy})_2\text{Ru}(\text{dpp})\text{Rh}^{\text{I}}(\text{bpy})]^{3+}$) (Fig. S12 and S13, ESI†). In $\text{Ru}^{\text{II}}\text{Rh}^{\text{III}}\text{Cl}(\text{tpy})$, Cl^- dissociation was also observed (Fig. S4, ESI†). Electrochemical reduction of the simple model $[\text{Rh}^{\text{III}}\text{Cl}(\text{tpy})\text{dpp}](\text{PF}_6)_2$ showed halide loss (Fig. S14, ESI†) to form $[\text{Rh}^{\text{I}}(\text{tpy})(\text{dpp})]^+$ ($m/z = 570.0$; calcd = 570.0, $M = [(\text{dpp})\text{Rh}^{\text{I}}(\text{tpy})]^+$) (Fig. S15, ESI†). The variable η^3 -tpy or η^2 -tpy coordination, of which the latter has been seen in some Re and Rh complexes,⁹ facilitates the necessary geometry change as Rh^{III} is reduced to Rh^{I} to form $[(\text{bpy})_2\text{Ru}(\text{dpp})\text{Rh}^{\text{I}}(\eta^2\text{-tpy})]^{3+}$. Additional support for the formation of $[(\text{bpy})_2\text{Ru}(\text{dpp})\text{Rh}^{\text{I}}(\eta^2\text{-tpy})]^{3+}$ is provided in the detailed photolysis studies of $\text{Ru}^{\text{II}}\text{Rh}^{\text{III}}\text{Cl}(\text{tpy})$. The addition of Cl^- to the photocatalytic system reduced H_2 production, whereas added tpy did not impact H_2 production, consistent with chloride, not tpy, loss occurring in the photocatalytic pathway. This η^2 -tpy gives steric protection on the Rh^{I} site and prevents deactivation of the catalyst by Rh^{I} dimerization.^{6b} Switching between η^2 and η^3 coordination at tpy provides a new mechanism to stabilize the supramolecule as it cycles the redox states at Rh in the catalytic cycle. Furthermore, one free pyridine of η^2 -tpy may assist catalysis through secondary coordination sphere effects.¹⁰ The improved functionality of $\text{Ru}^{\text{II}}\text{Rh}^{\text{III}}\text{Cl}(\text{tpy})$ over $\text{Ru}^{\text{II}}\text{Rh}^{\text{III}}\text{Cl}_2(\text{bpy})$ results from the enhanced driving force for reductive quenching by DMA, the rapid rate of halide loss and the steric protection of the photogenerated Rh^{I} imparted by the tpy ligand.^{4g,6b}

In conclusion, a new photocatalyst, $\text{Ru}^{\text{II}}\text{Rh}^{\text{III}}\text{Cl}(\text{tpy})$, with one Cl ligand and a tridentate ligand on the Rh^{III} center has shown light-driven H_2 production from water. This established that two labile halide ligands on the Rh^{III} center are not mandatory for photocatalysis. The replacement of one halide with a pyridyl ligand successfully increases the rate of halide loss and the E_{redox} for reductive quenching of the $^3\text{MLCT}$ excited state by DMA. Increased driving force for intramolecular electron transfer from reduced dpp to Rh also increases photocatalytic efficiency. This study shows that photocatalytic activity can be controlled by tuning the Rh redox properties and demonstrates a new approach to design photocatalysts for H_2 generation.

Acknowledgements were made to Professor Paul A. Deck for his helpful discussion and the Chemical Sciences, Geosciences and Biosciences Division, Office of Basic Energy Sciences, Offices of Sciences, U.S. Department of Energy DE FG02-05-ER15751 for financial support.

Notes and references

- (a) D. G. Nocera, *Acc. Chem. Res.*, 2012, **45**, 767–776; (b) T. S. Teets and D. G. Nocera, *Chem. Commun.*, 2011, **47**, 9268–9274; (c) N. Armaroli and V. Balzani, *ChemSusChem*, 2011, **4**, 21–36; (d) N. S. Lewis and D. G. Nocera, *Proc. Natl. Acad. Sci. U. S. A.*, 2006, **103**, 15729–15735; (e) A. J. Bard and M. A. Fox, *Acc. Chem. Res.*, 1995, **28**, 141–145.
- (a) V. Balzani, L. Moggi, M. F. Manfrin, F. Bolletta and G. S. Laurence, *Coord. Chem. Rev.*, 1975, **15**, 321–433; (b) V. Balzani, L. Moggi and F. Scandola, in *Supramolecular Photochemistry*, ed. V. Balzani, Reidel, Dordrecht, 1987, vol. 214, pp. 1–28.
- J. M. Lehn and J. P. Sauvage, *Nouv. J. Chim.*, 1977, **1**, 449–451.



- 4 (a) H. Ozawa, M. Haga and K. Sakai, *J. Am. Chem. Soc.*, 2006, **128**, 4926–4927; (b) S. Rau, B. Schafer, D. Gleich, E. Anders, M. Rudolph, H. Friedrich, W. Gorts, J. G. Henry and J. G. Vos, *Angew. Chem., Int. Ed.*, 2006, **118**, 6215–6218; (c) S. Jasimuddin, T. Yamada, K. Fukujū, J. Otsuki and K. Sakai, *Chem. Commun.*, 2010, **46**, 8466–8468; (d) A. Fihri, V. Artero, M. Razavet, C. Baffert, W. Leibl and M. Fontecave, *Angew. Chem., Int. Ed.*, 2008, **47**, 564–567; (e) P. Zhang, M. Wang, C. Li, X. Li, J. Dong and L. Sun, *Chem. Commun.*, 2010, **46**, 8806–8808; (f) M. Elvington, J. Brown, S. M. Arachchige and K. J. Brewer, *J. Am. Chem. Soc.*, 2007, **129**, 10644–10645; (g) T. A. White, B. N. Whitaker and K. J. Brewer, *J. Am. Chem. Soc.*, 2011, **133**, 15332–15334; (h) T. Stoll, M. Gennari, J. Fortage, C. E. Castillo, M. Rebarz, M. Sliwa, O. Poizat, F. Odobel, A. Deronzier and M.-N. Collomb, *Angew. Chem., Int. Ed.*, 2014, **53**, 1654–1658; (i) T. Stoll, C. E. Castillo, M. Kayanuma, M. Sandroni, C. Daniel, F. Odobel, J. Fortage and M.-N. Collomb, *Coord. Chem. Rev.*, DOI: 10.1016/j.ccr.2015.02.002.
- 5 (a) S. M. Arachchige, J. Brown, R. E. Chang, A. Jain, D. F. Zigler, K. Rangan and K. J. Brewer, *Inorg. Chem.*, 2009, **48**, 1989–2000; (b) T. A. White, S. L. H. Higgins, S. M. Arachchige and K. J. Brewer, *Angew. Chem., Int. Ed.*, 2011, **50**, 12209–12213; (c) T. A. White, J. D. Knoll, S. M. Arachchige and K. J. Brewer, *Materials*, 2012, **5**, 27–46; (d) G. F. Manbeck and K. J. Brewer, *Coord. Chem. Rev.*, 2013, **257**, 1660–1675; (e) T. A. White, K. Rangan and K. J. Brewer, *J. Photochem. Photobiol., A*, 2010, **209**, 203–209.
- 6 (a) M. Elvington and K. J. Brewer, *Inorg. Chem.*, 2006, **45**, 5242–5244; (b) J. Wang, T. A. White, S. M. Arachchige and K. J. Brewer, *Chem. Commun.*, 2011, **47**, 4451–4453.
- 7 D. F. Zigler, J. Wang and K. J. Brewer, *Inorg. Chem.*, 2008, **47**, 11342–11350.
- 8 T. A. White, S. M. Arachchige, B. Sedai and K. J. Brewer, *Materials*, 2010, **3**, 4328–4354.
- 9 (a) H. Aneetha, P. S. Zacharias, B. Srinivas, G. H. Lee and Y. Wang, *Polyhedron*, 1998, **18**, 299–307; (b) Q. Ge, T. C. Corkery, M. G. Humphrey, M. Samoc and T. S. A. Hor, *Dalton Trans.*, 2009, 6192–6200.
- 10 (a) J. Y. Yang, S. E. Smith, T. Liu, W. G. Dougherty, W. A. Hoffert, W. S. Kassel, M. R. Dubois, D. L. Dubois and R. M. Bullock, *J. Am. Chem. Soc.*, 2013, **135**, 9700–9712; (b) G. E. Dobereiner, A. Nova, N. D. Schley, N. Harari, S. J. Miller, O. Eisenstein and R. H. Crabtree, *J. Am. Chem. Soc.*, 2011, **133**, 7547–7562.

